Dynamic analysis of anchored concrete linings of plunge pools loaded by high velocity jet impacts issuing from dam spillways

Maziar Mahzari
MWH Sydney
39-41 Chandos Street
St Leonards
NSW 2065
Australia
Email: maz.mahzari@au.mwhglobal.com

Anton J Schleiss
Full Professor
Laboratory of Hydraulic Constructions (LCH)
École Polytechnique Fédérale de Lausanne (EPFL)
Station 18
CH-1015 Lausanne
Switzerland
Email: anton.schleiss@epfl.ch

Abstract

A theoretical stochastic approach is presented for the structural analysis of plunge pool liners dynamically loaded by the impact of free-falling jets. Such an approach was used as the real behaviour of plunge pool liners is complex, and deterministic methods usually fail to represent the true response of the system. This general approach can easily be used in design practice, given the random characteristics of the loading. Based on the pressure fluctuations measured in the laboratory under prototype conditions, a general model for the stochastic loading of the liner is established. Using simplified random analysis, dynamic magnification factors are calculated as a function of the design load level and safety margin. The results indicate sensitivity of the magnification factor regarding the transient loading characteristics, as mainly the frequency content, which are not taken into account in classic deterministic approaches. Furthermore, the influence of the structural properties of the anchored plunge pool lining on the response is also studied.

Keywords: Plunge pool liner, high velocity jets, dynamic uplift, liner anchorage, pressure fluctuation, stochastic analysis.

1. Introduction

Downstream of dams the energy of free-falling water has to be controlled, often by dissipating structures, in order to prevent progressive scouring which can endanger the stability of the foundations. Examples of such energy control structures are stilling basins and plunge pools. In stilling basins, the energy of high velocity flow is dissipated within a hydraulic jump. Normally, therefore, no severe scour is expected downstream of the lined stilling basin in the case of a rocky river bed. Plunge pools are widely used to dissipate the energy of free-falling jets created by free overflow or orifice spillways of dams. Plunging of jets into deep pools significantly reduces their scour potential. However, when the depth of the plunge pools is not sufficient, undesirable scouring is expected. In this situation concrete linings may be used to protect the plunge pool bottom against the high energy impact of the jet, as scoured areas can endanger the stability of the dam foundation.

The flow pattern in plunge pools is characterised by large eddies in various regions, as well as high turbulent flow near the impact area of the jet. The latter results in high fluctuating pressures acting on the plunge pool bottom. In the case of concrete lined plunge pools, the liner is in this case subjected to considerable dynamic uplift pressures. This may result in large displacements, or even rupture of the lining, if it is not properly anchored to the rock.

Well defined methodologies are rarely found for the assessment of dynamic loading of the concrete linings of plunge pools. Often the results of the physical models are used for loading assessment. However, due to the scale effects, the dynamic loading of the prototype cannot be fully represented. An appropriate design procedure should consider two major aspects of the system behaviour:

- Definition of the dynamic loading in order to take into account its stochastic nature.
- Proper modelling of the liner so that its response to the loading is sufficiently estimated.

Pressure fluctuations due to turbulence have been assessed by various research studies. Xu *et al* [19], Castillo [7], and Pinheiro [15] have studied stochastic characteristics of the pressure fluctuations on the floor of plunge pools. More recently, Pinheiro *et al* [16] also described the effect of jet aeration on hydrodynamic forces on plunge pool floors. Armengou *et al* [1], and Ramos & Melo [17], measured the correlation of spatial pressure distribution over the plunge pool bottom, and observed weak spatial correlation for pressure fluctuations.

Uplift pressure peaks at plunge pool liners were reported by Kirschke [11]. These peaks were significantly higher than the mean dynamic underpressure also shown in the more recent work of Bollaert [3, 4, 5]. Yuditskii [20] had already studied this phenomenon, and concluded that these high uplift peaks do not endanger the instability of the liner due to their short duration. Lyatkher & Khalturina [12] measured the transmission

of the pressure fluctuations under a slab, and studied its correlation with the width of the joints. Mirtskhulava *et al* [14] studied the pressure induced vibrations of the slab, and their effects on its foundation. Some deterioration resulting from the vibration of the liner was reported. The effect of the joint width on the dynamic uplift was studied by Townson [18].

Most of the aforementioned cited works were oriented towards the analysis of the pressure fluctuations and their stochastic characteristics. Nevertheless, none of the studies give practical design recommendations for anchor bolts.

Fiorotto & Salandin [8] have made the following assumptions to evaluate the loading and response of the liner of a stilling basin:

- The waterstops fail during operation, and the dynamic uplift is created underneath the anchored slab.
- The temporal distribution of the pressure under the slab is exactly the same as the pressure above the slab.
- Structural properties of the slab are determined based on the amount of anchorage of the slab.
- The pressure fluctuation time history is a stationary and ergodic random process.
- Spatial distribution of the pressure on the slab is idealised by an averaging process and a constant factor, (Ω), is used to remove the space coordinates.
- Submerged density for the concrete slab is considered to account for the static uplift pressure.

Applying the persistence time concept for the fluctuations, Fiorotto & Rinaldo [9] modelled the slab system as a single degree of freedom system (SDOF). The load is introduced as a step function, which results in an amplification factor of two for the forces in the anchor bolts if the persistent time is long enough. Based on these results, it was recommended that the area of anchor bolts should be doubled for a safer design. Fiorotto & Rinaldo [9] considered a full correlation between the pressure above and underneath the slab, which means they are identical. Obviously the evolution pressure development underneath the slab is much more complex. Therefore, to be more realistic, a correlation function between the pressure above and underneath the slab should be introduced. This function statistically identifies how the pressure loadings amplify and/or cancel each other out. Another improvement would be to include the frequency content of the loading, which can offer a better solution for the system.

Bollaert [6] proposed to calculate the dynamic uplift pressure under the slab with a numerical model, for the transient flow in the joints with various air concentrations. Consequently, knowing the pressure distribution above and underneath the slab, the system may be dynamically analysed for the applied loadings. According to Bollaert [6], spatial distribution of the instantaneous pressure loading on the slab can be included in

the analysis. However, as the pressure fluctuations above the slab behave stochastically, such a deterministic approach requires significant computing time, and is difficult to apply in practice. Melo *et al* [13] used a formula for dynamic pressures across the impinging developed jet, according to Häusler [10], to evaluate the stability of the liner slabs. Uplift pressures are evaluated from the above pressure distribution. The Colebrook-White formula is used for calculation of the head losses along the joints in the lining and the liner-foundation contact. In this static analysis, the time varying pressure fluctuations are not considered.

In the present paper a general approach for the design of the required anchor forces, considering dynamic effects and correlation of pressures acting above and underneath the concrete slab, is presented. The description and interpretation of the pressure fluctuations itself will not be addressed, since it has already been covered in the aforementioned literature.

2. Dynamic loading of anchored concrete liner by pressure fluctuations

Figure 1 indicates a schematic representation of an anchored reinforced concrete slab, loaded by pressure fluctuations.

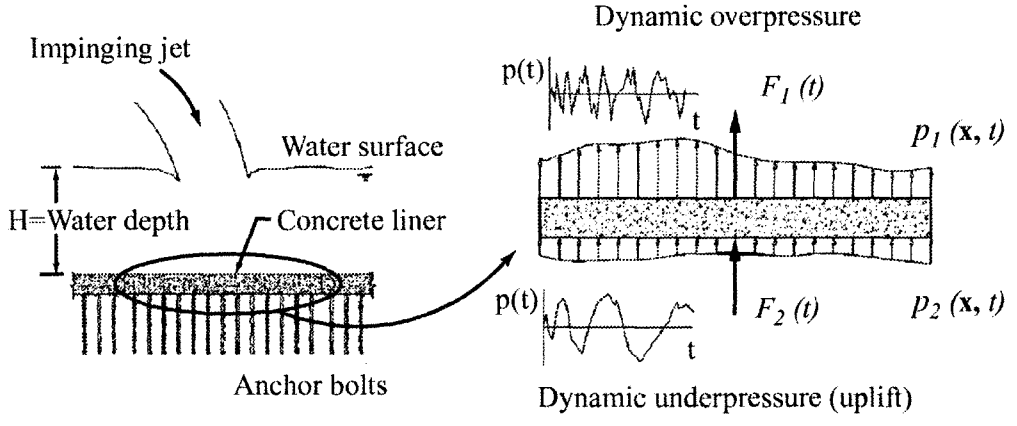

Figure 1. *Schematic representation of an anchored concrete slab, and the dynamic pressure loading*

Normally the whole liner is divided into segments, or slabs, separated by construction joints. The dimension of the slabs depends on the size of the lined area, thermal conditions, construction considerations, and other parameters. The joints between the slabs are usually protected with double waterstops, the purpose of which is to prevent penetration of the pressure fluctuations under the slab, which increases the dynamic uplift forces.

The concrete slabs have to be anchored by simple rock bolts, or pre-stressed tendons, in order to withstand dynamic uplift.

It is probable that the waterstops will fail due to the high pressure load of the water jet, or be damaged during construction. Therefore, a realistic design scenario is to assume that the waterstops have failed, and pressure fluctuations are transferred underneath the slab through the construction joints.

While the pressure fluctuations travel through the joints and under the slab, the characteristics of the pressure field change for various reasons. Firstly, the pressure wave is transferred through the joints, and is reflected when it reaches the other end of the joint. Secondly, the pressure developed underneath the slab also propagates in the fissured rock supporting the liner. The combination of the developed pressure field, reflection and resonance effects, as well as pressure wave propagating in the rock, creates a very complicated loading underneath the slab, which is called dynamic uplift.

The properties of dynamic uplift pressures are highly dependent on the joint configuration, the anchorage system of the slab, and the properties of the rock supporting the lining.

Pressure fluctuations above and beneath the slab have a random behaviour due to dominating turbulence in the flow pattern, and the propagating pressure wave underneath the slab, respectively. Therefore, a stochastic approach is the best way to properly describe the dynamic loading. In such an approach the uncertainty level in the loading, and the response of the slab, is quantified by analytical methods.

3. Analysis of anchored concrete linings loaded by pressure fluctuations

For the dynamically loaded liner shown in Figure 1, the net uplift force is normally higher than the self weight of the liner slabs. Therefore, in practice, the liner slabs have to be anchored by means of rock bolts or pre-stressed tendons. Due to the dynamic nature of the loading, the slab anchor system will have a vibrating response. In Section 3.1. the uplift loads for which the anchors have to be designed is evaluated.

3.1. Modelling pressure fluctuation loading

The loading can be fully defined by the pressure fluctuations above and underneath the liner. However, there is no theoretical method to directly obtain these loads from the hydraulic characteristics of the jet. Nevertheless, the pressure fluctuations can be derived from measurements on a physical scaled model, or possibly a prototype.

It is known that these transients are near ergodic-stationary processes [2, 9, 19], therefore they can be modelled appropriately by PSDs (Power Spectral Density functions) [3], which are frequency interdependent functions.

The required PSD functions are denoted as overpressure force PSD, $S_{F_1}(\omega)$, underpressure force PSD, $S_{F_2}(\omega)$, and the cross-correlation PSD between the pressure force above and underneath the slab, $S_{F_1F_2}(\omega)$, and $S_{F_2F_1}(\omega)$. Having high quality measurement results, these functions can be obtained by means of a numerical spectral analysis.

According to, and considered by Bollaert [6], the overpressure fluctuation may also be transferred inside the fissures, and considered by a transfer function derived theoretically. The major effect of the joints is to filter a range of frequencies from the dynamic uplift underneath the slabs, and to change the characteristics of the transient pressure acting on the slabs.

In the laboratory, Bollaert & Schleiss [5] measured the dynamic characteristics for plunging jets at high velocity, as they would occur in a prototype. PSD functions were measured for different cases [3]. Although the derived PSD functions cannot be directly considered without scaling for analysis, they can provide a good basis for the selection of the model, and the sensitivity analyses.

3.2. Structural model of the system

The response of the anchored liner is non-linear due to the stiffness variations. While the anchors are in tension, the stiffness is provided only by them. However, when the liner is pushed onto the rock support (complete contact with the underlying rock), the stiffness is provided by the rock foundation, and the stiffness of the anchors is negligible. For a deterministic load, a non-linear dynamic analysis can be used to obtain the response time history. However, such an analysis cannot be used in engineering practice due to the uncertainties of the loading.

The system can be simplified as a single degree of freedom system (SDOF) due to the high rigidity of the slab. Other authors, such as Fiorotto & Bollaert [6, 8, 9], have also assumed a linear stiffness for the SDOF, based on the stiffness of the anchors. This approximation may be improved by using an equivalent SDOF, in which the non-linear response is approximated by an equivalent linear system, taking into account the non-linear stiffness and energy dissipation associated with the interaction effects.

To define the equivalent linear system, a non-linear dynamic analysis of the SDOF could be performed. The stiffness of the anchors (with an effective length) is used for positive (anchors in tension) displacement. For negative displacements, i.e. when the rock introduces stiffness into the system, the impedance function of an infinite elastic media for a rectangular foundation is used. Such harmonic analysis has to be conducted for various excitation frequencies and load amplitudes. Figure 2 illustrates the model used. As an example the results of a non-linear analysis, as well as the equivalent linear system, is given. Based on the dissipated energy per cycle, and maximum displacement when the anchors are under tensile stresses, it is conservatively normalised.

It can be seen that assuming an equivalent stiffness, based on the stiffness of anchors, is a realistic and conservative assumption. However, a specific amount of damping should also be implemented in the model.

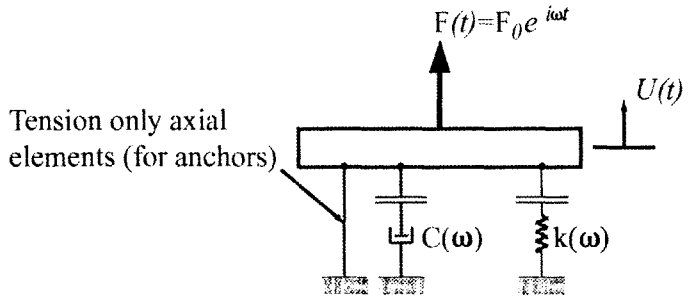

(a)

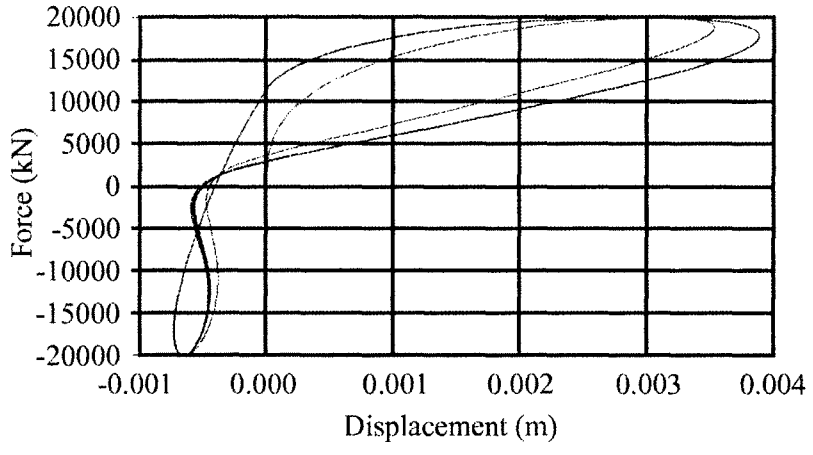

(b)

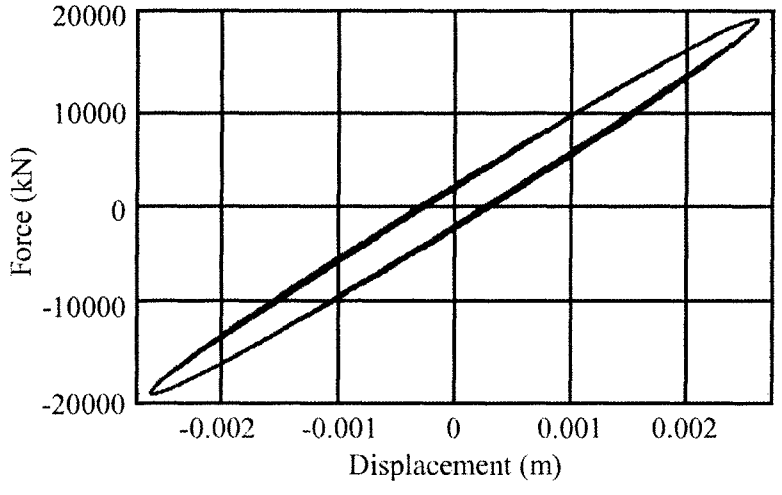

(c)

Figure 2. *(a) The real SDOF model, (b) a genuine sample force displacement curve, and (c) equivalent SDOF force displacement curve*

3.3. Analysis procedure

For a linear SDOF subjected to two different loadings, ($F_1(t)$ and $F_2(t)$), with different spectral properties, the response can be determined by:

$$u(t) = \int_{-\infty}^{\infty} h(\theta)\, F_1(t - \theta)\, d\theta + \int_{-\infty}^{\infty} h(\theta)\, F_2(t - \theta)\, d\theta \qquad (1)$$

where $h(\theta)$ is the impulse response function which depends on the physical properties of the SDOF, namely mass, damping, and stiffness (m, c_e, and k_e).

Assuming zero for the input motions, the variable that characterises stochastic response of u is its PSD and RMS (Root Mean Square), which can be calculated from the PSD.

Knowing the frequency response function for u ($H(\omega)$), its PSD can be obtained by:

$$S_u(\omega) = |H(\omega)|^2 [S_{F_1}(\omega) + S_{F_1F_2}(\omega) + S_{F_2F_1}(\omega) + S_{F_2}(\omega)] \qquad (2)$$

The RMS value of the displacement, σ_u, is then calculated:

$$\sigma_u = \sqrt{\int_{-\infty}^{\infty} |H(\omega)|^2 [S_{F_1}(\omega) + S_{F_1F_2}(\omega) + S_{F_2F_1}(\omega) + S_{F_2}(\omega)] d\omega} \qquad (3)$$

Having established the power spectral density and the cross-spectral density functions, the PSD function of the vertical displacement of the liner and its RMS value are easily derived. Assuming a classic normal distribution for the displacement, the stochastic response of the liner is completely defined by:

$$U_{\max} = C_r\, \sigma_u \qquad (4)$$

where C_r is the factor associated with the level of acceptable risk in the design.

The dynamic component of the anchor force has to be superimposed with the static component (knowing the submerged weight of the liner), to obtain the required design anchor force. Obviously the design is a trial and error procedure, in which the required number of anchors is not known from the beginning.

4. Practical applications

For practical applications, the most important issue is modelling and defining the acting dynamic pressures.

Pressure measurements and analysis performed by Bollaert [3] for core and developed jets with prototype velocities can be used as PSD functions. However, when determining the loading from these results, the following has to be considered:

• The results from the model tests have to be scaled properly. Froude scaling is recommended, however, even if there are some doubts regarding its validity for scaling the frequency to pressure fluctuations and its PSD function. Therefore, a near prototype scale model offers more realistic results. In any case, it is recommended to use a sensitivity analysis for engineering practice, which provides a more appropriate basis for design.

• The studies of Melo *et al* [13] indicate a weak spatial correlation for the pressure fluctuations at the bottom of the plunge pool. Therefore the use of a spatial averaging coefficient (Ω), as proposed by Fiorotto & Rinaldo [9], seems to be realistic. Using this factor, total force PSD can be derived directly from an average pressure PSD. However, the proposed approach in this paper is even applicable to correlated pressure fluctuations. With the use of a multi degree of freedom system (MDOF) for the liner, the spatial pressure fluctuations and their correlations can be included properly.

4.1. Analysis of impervious plunge pool liners

As a reference case an impervious plunge pool liner is analysed, and then the loading is modelled. Figure 3a shows the reproduced PSD functions for the pressure fluctuations measured by Bollaert [3] for a developed jet normalised to its RMS value. It can be seen that the PSD functions have the same general shape for various incoming jet energy. It can be approached by a general bi-linear form for the PSD function of the force in the logarithmic scale, as shown in Figure 3b. The PSD model is fully specified with three frequency values (ω_1, ω_2 and ω_3), two exponential values (n_1 and n_2), and a predefined RMS for pressure loading. The function is assumed to be zero for a frequency below ω_1 and above ω_3. The initial and decay exponents are considered to be $n_1 = -1$, and $n_2 = -7/3$, as suggested by Bollaert [3].

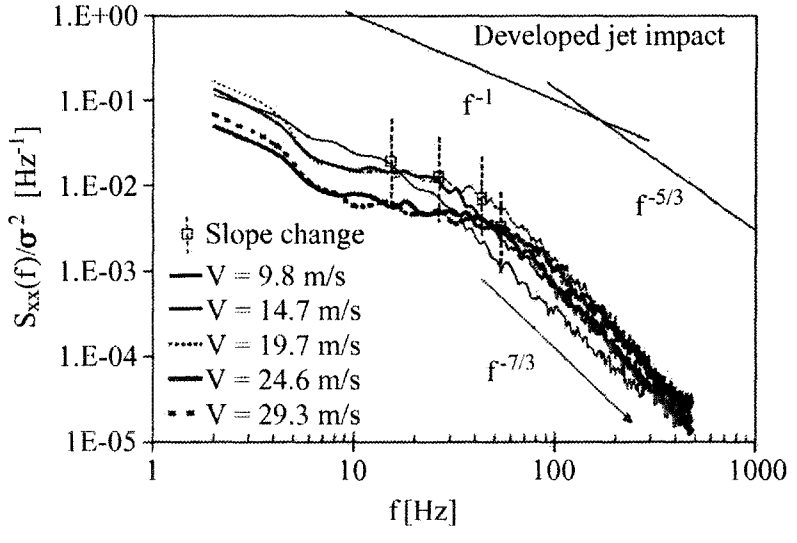

(a)

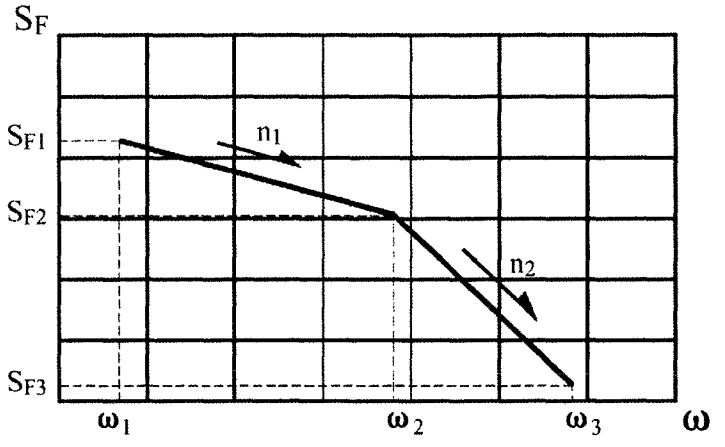

(b)

Figure 3. *General form of force PSD function, (a) measured values, and (b) proposed loading model*

The three frequency values (ω_1, ω_2 and ω_3) are the initial frequency, the point of change of slope frequency, and the cut-off frequency. The frequency values measured by Bollaert [3] are approximately $\omega_1 = 2\pi$ x 0.1rad/sec, $\omega_2 = 2\pi$ x 25rad/sec, and $\omega_3 = 2\pi$ x 500rad/sec ($f_1 \approx 0.1$Hz, $f_2 \approx 25$Hz, and $f_3 \approx 500$Hz). High component frequencies have only a small contribution to the PSD. Depending on the scale of the model, these frequency values are reduced by $(1/s)^{1/2}$ factor, where s is the scale of the model. For three assumed scales, Table 1 includes the frequencies of the measured pressures.

Scale	ω_1	ω_2	ω_3
1:1	2π x 0.1(rad/sec)	2π x 25(rad/sec)	2π x 500(rad/sec)
1:5	2π x 0.04(rad/sec)	2π x 11(rad/sec)	2π x 224(rad/sec)
1:10	2π x 0.03(rad/sec)	2π x 8(rad/sec)	2π x 158(rad/sec)
1:20	2π x 0.02(rad/sec)	2π x 6(rad/sec)	2π x 112(rad/sec)

Table 1. *Frequency range for different assumed scales of the model*

The high frequency components may be attributed to the small turbulent flow patterns, which are negligible if the averaging of the pressure is used for the evaluation of the PSD function of the net force on the liner. These components have a very low contribution to

the force PSD function. Nevertheless, before the spatial correlation over the slab is completely known, it would be dangerous to modify the force PSD function and filter out these high frequency components. Therefore these high frequency components should be included in the design.

Spectral density values (S_{F1}, S_{F2} and S_{F3}) are obtained by normalising the area under the PSD function to the RMS of the loading. The assumed RMS is the spatially averaged value. This means that the maximum pressure is reduced by Ω factor to account for the non-uniform pressure distribution on the liner.

Figure 4 indicates the normalised PSD and its associated auto-correlation function of the net force for σ_p = 50kPa (RMS value), n_1 = -1, n_2 = -7/3, $\omega_1 = 2\pi$ x 0.1rad/sec, $\omega_2 = 2\pi$ x 25rad/sec, and $\omega_3 = 2\pi$ x 500rad/sec.

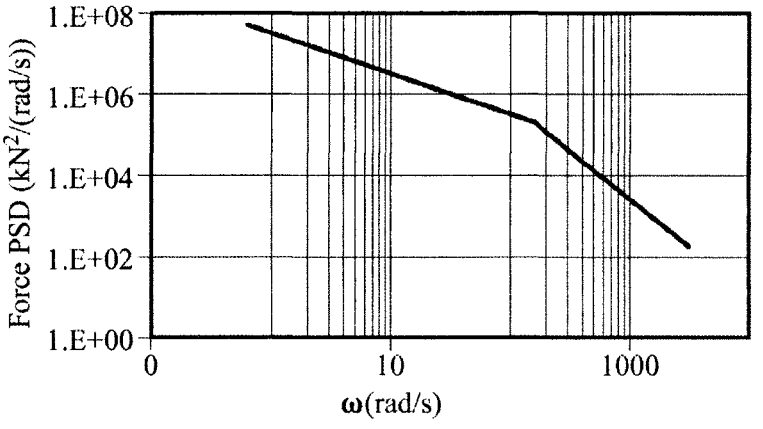

(a)

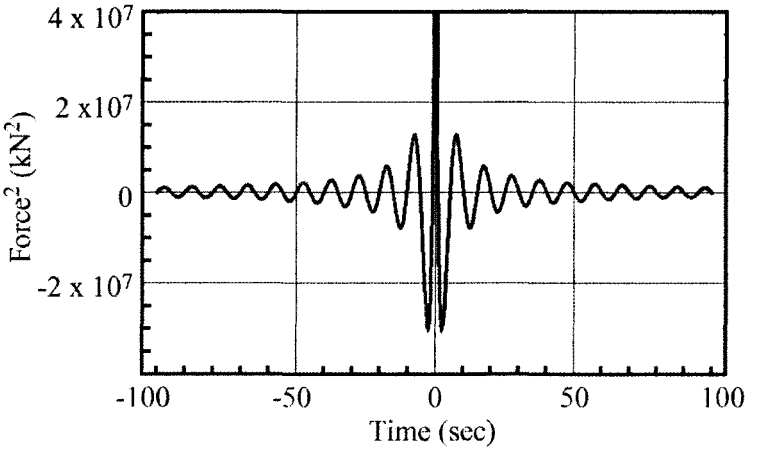

(b)

Figure 4. *(a) PSD function, and (b) auto-correlation function of the pressure fluctuations*

Using Equation 3, the maximum displacement of the liner is:

$$u_{max} = C_r \sqrt{2\left[\int_{\omega_1}^{\omega_2} \frac{a_1\,\omega^{n_1}}{(k_e - m\omega^2)^2 + (c_e\omega)^2}\,d\omega + \int_{\omega_2}^{\omega_3} \frac{a_2\,\omega^{n_2}}{(k_e - m\omega^2)^2 + (c_e\omega)^2}\,d\omega\right]} \qquad (5)$$

where a_1 and a_2 are constant terms of each line segment of the loading PSD function, calculated from the given data.

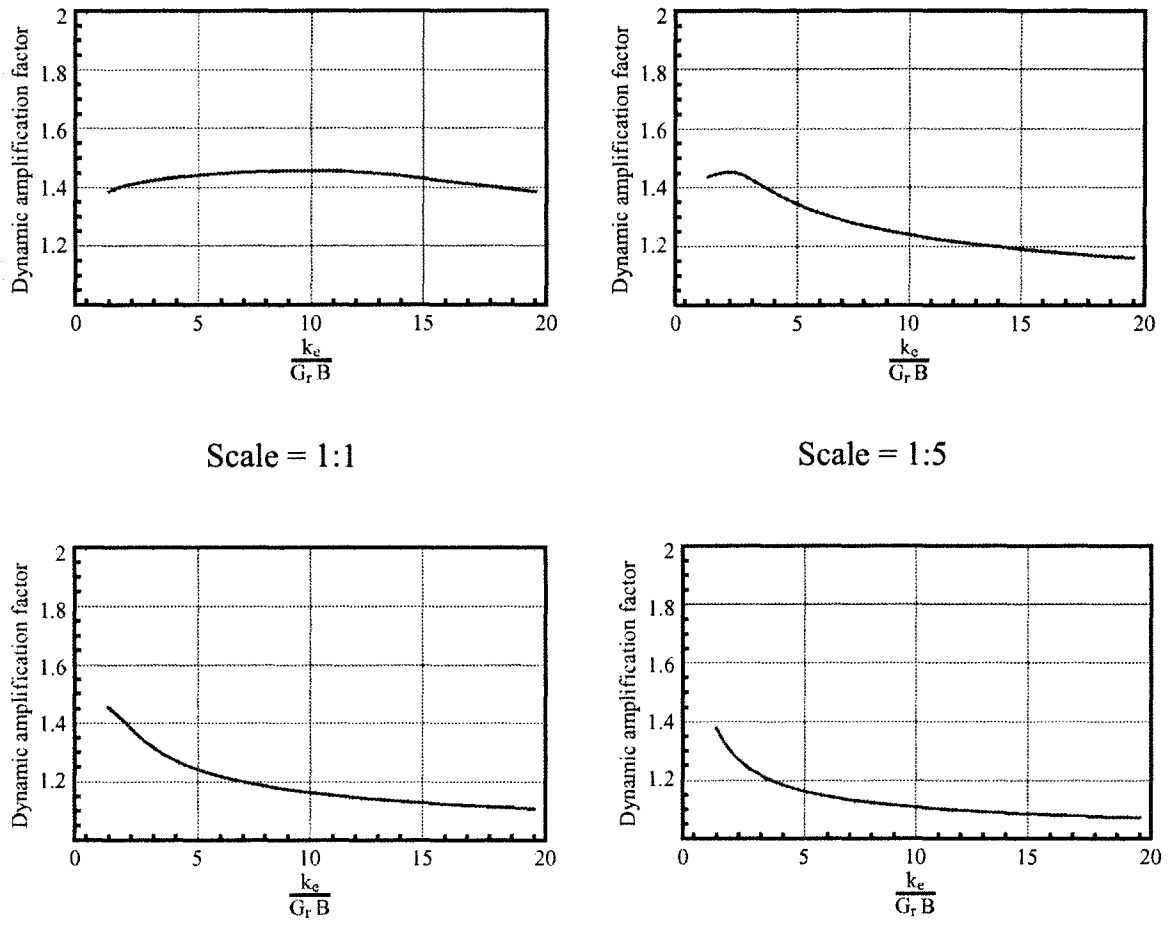

Figure 5. *Amplification factor for various normalised stiffness values, ($k_e/G_r B$), and scales of an impervious liner*

In the following, the proposed procedure is illustrated by an application. A square liner segment 20m x 20m (2B = 20m), 2m thick, located on a rock foundation with elastic properties E_r = 1GPa, ν_r = 0.28 (G_r = 0.391GPa) and ρ_r = 1.80ton/m^3, is analysed for

the pressure fluctuation loading represented by the PSD shown in Figure 4, with frequency ranges given in Table 1.

The liner is secured to the rock with 144 anchors, each 32mm in diameter, and 10m long (spacing between the anchors is approximately 1.5m). For E_{steel} = 2.068 x 10^5MPa, and an effective length of L_e = 0.25m x 10m = 2.5m, the stiffness of the system considering anchors would be 9.58GN/m (normalised k_e = 9.85/(0.391 x 10) = 2.45).

Assuming the rock foundation as an elastic half space, the impedance function for a rigid rectangular foundation is available, and is used for calculation of the response. It should be noted though that the stiffness depends on the frequency, and hence a sensitivity analysis has to be carried out.

Using non-linear dynamic analysis, equivalent damping of the system can be calculated. For the above example a minimum value of ξ = 10.64%, corresponding to 10πrad/sec average frequency, was obtained. Comparing the dynamic with the static force in the anchors (static force depending only on the loading and number of anchors), the amplification factor is calculated as the ratio of the dynamic to the static anchor forces. Figure 5 shows the variation of the dynamic amplification factor (DA) as a function of normalised equivalent stiffness (k_e/G_R·B), where G_r is the rock foundation elastic shear modulus.

As can be clearly seen the dynamic amplification, compared to the static loading, cannot be neglected (in minimum 20% amplification). Ignoring this dynamic effect would mean that the amount of required anchoring steel would be underestimated.

4.2. Analysis of pervious plunge pool liners

In the case of a pervious plunge pool liner, dynamic uplift occurs. The problem can be easily solved if the PSD functions of Equation 2 are known. Some simplified cases are illustrated in the following.

4.2.1. Equal dynamic pressure above and underneath the slabs

If dynamic pressure above and underneath the slabs is identical, Equations 3 and 4 are combined and simplified as:

$$u_{\max} = C_r \sqrt{2\left[\int_{\omega_1}^{\omega_2} \frac{a_1\,\omega^{n_1}}{(k_e - m\omega^2)^2 + (c_e\omega)^2}\,d\omega + \int_{\omega_2}^{\omega_3} \frac{a_2\,\omega^{n_2}}{(k_e - m\omega^2)^2 + (c_e\omega)^2}\,d\omega\right]} \qquad (6)$$

which is twice the value given in Equation 5, as expected. However, it should be noted that the force in the anchors is not linear, due to the superposition of the dynamic forces with the self weight of the liner.

Figure 6 shows the sensitivity of the dynamic amplification factor (DAF) as a function stiffness of the different scale system.

Comparing the results for the pervious and impervious liners, it can be seen that the dynamic amplification factor is almost identical.

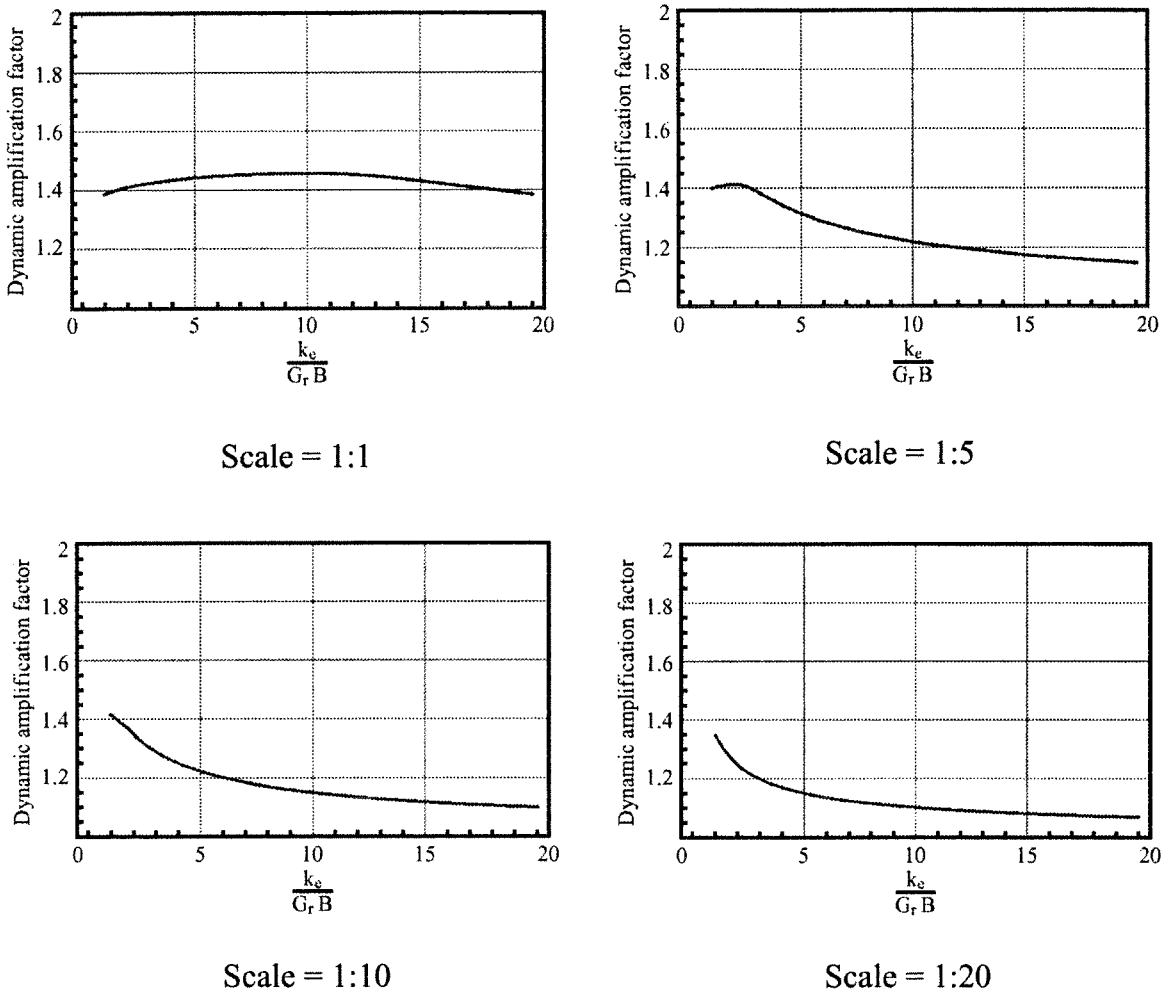

Figure 6. *Amplification factor for various normalised stiffness values, and scales of a pervious liner*

4.2.2. Lagged dynamic uplift

Another assumption is that the dynamic uplift is equal to the pressure above the slab, but with a lag time (T). This means that the joints have no effect on the characteristics of the fluctuations, and the pressure above the slab is transferred under the liner with a lag time.

For the lag time, T, Equation 3 is simplified as:

$$\sigma_u = \sqrt{\int_{-\infty}^{+\infty} |H(\omega)|^2 \{2\, S_F(\omega)\,[1 + \cos(\omega T)]\}\, d\omega} \qquad (7)$$

where $S_F(\omega)$ is the PSD function given in Figure 4. The maximum displacement is:

$$u_{max} = C_r \sqrt{2\left[\int_{\omega_1}^{\omega_2} \frac{2a_1\,\omega^{n1}\,[1+\cos(\omega T)]}{(k_e - m\omega^2)^2 + (c_e\omega)^2}\,d\omega + \int_{\omega_2}^{\omega_3} \frac{a_2\,\omega^{n2}\,[1+\cos(\omega T)]}{(k_e - m\omega^2)^2 + (c_e\omega)^2}\,d\omega\right]} \quad (8)$$

Figure 7 gives the amplification factor as a function of the pressure time lag, T, between pressure above and underneath the slab (in seconds) for different scales.

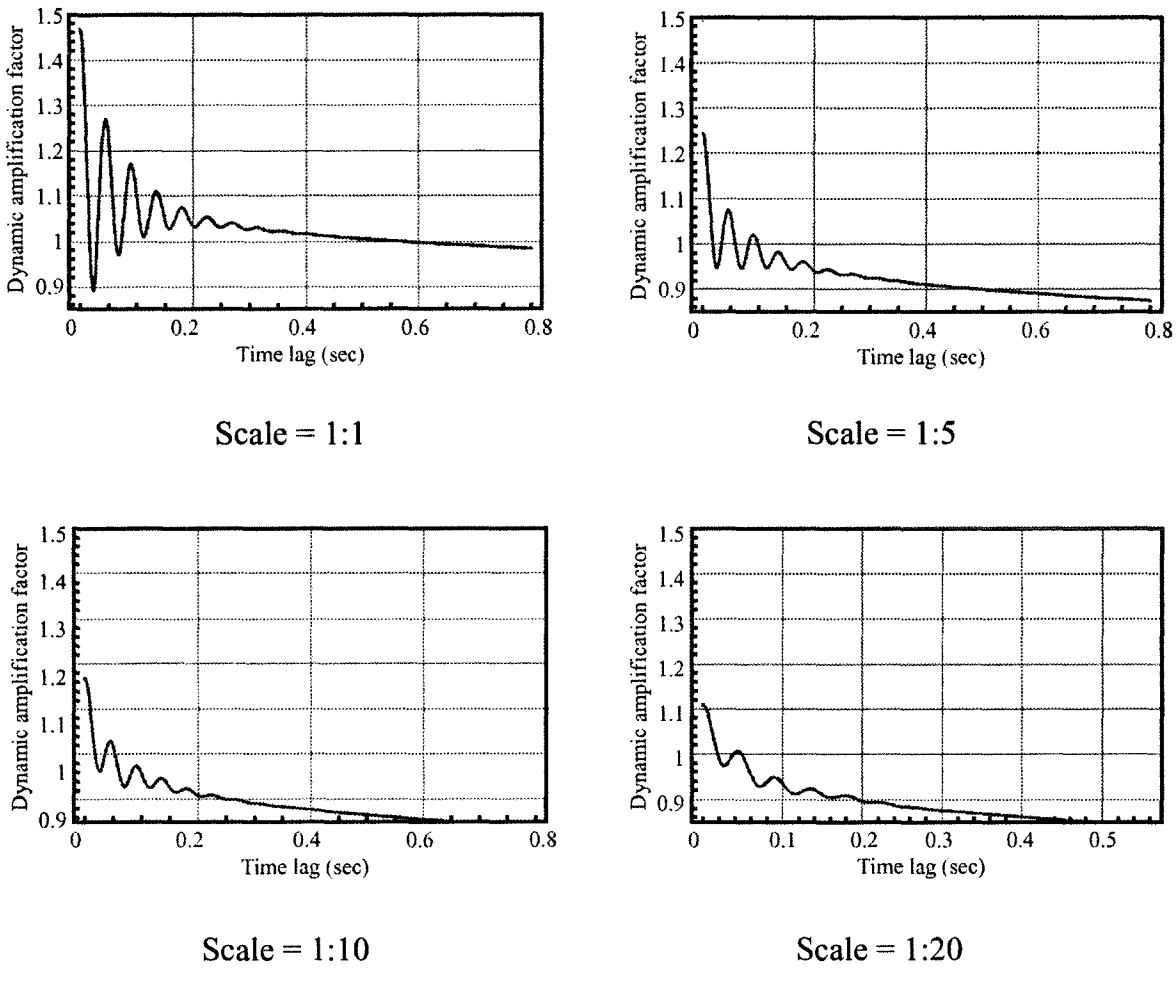

Figure 7. *The dynamic amplification factor as a function of the time lag (sec) between the dynamic pressure above and underneath the slab for different scales*

Maximum amplification occurs when there is no time lag between the dynamic pressures above and underneath the slabs. With an increase in the time lag, and after oscillating behaviour (due to the presence of the $\cos(\omega T)$ term), the amplification factor is reduced. For Scale = 1:1, which is the most severe case, as expected ($DAF_{max} = 1.46$), the amplification factor drops below 1.0 for a time lag of approximately 0.55sec, and dynamic effects can be ignored completely (the static uplift can be used for the design of the

anchorage amount). The assumed time lag is generally a function of the speed of travel of the fluctuation waves through the joints and underneath the slab, and a characteristic length of the travel of the waves. If this is assumed to be from the centre of the slab at the top surface, to the centre of the slab at the bottom surface (approximately equal to the slab segment dimension), then one can calculate the approximate lag time knowing the speed of the wave. For the slab segment with a 20m dimension, assuming a wave speed of between 100~500m/sec in the water (and the presence of small bubbles), the lag time is about 0.04~0.2sec. This time lag barely produces dynamic effects for cases other than the 1:1 scale (the high frequency loading), and a dynamic amplification factor of a maximum of 1.25 is observed.

4.2.3. Constant-banded dynamic uplift

Assuming a constant PSD over a frequency range may result in an upper boundary for the dynamic amplification factor. This pressure fluctuation could be represented by a central frequency (ω_c) with a specific bandwidth ($\Delta\omega$,) as shown in Figure 8. Knowing the RMS of the pressure fluctuations, the area under the PSD can be normalised.

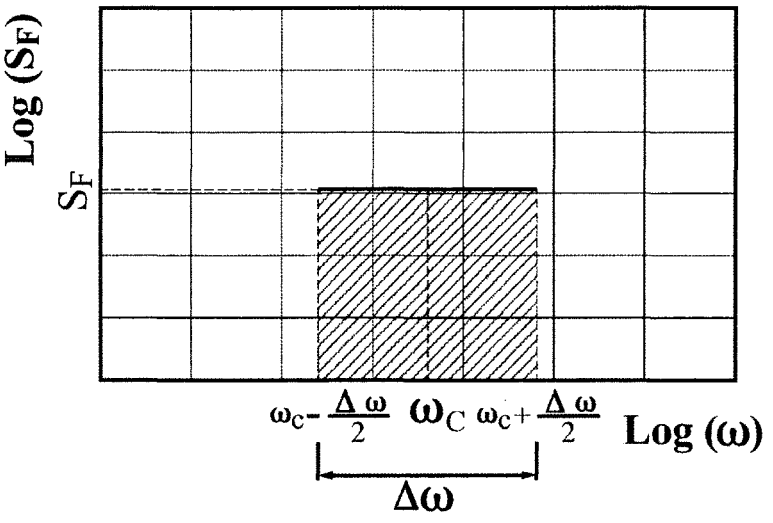

Figure 8. *Constant-banded PSD for dynamic under-pressure*

Theoretically, this PSD would be interpreted as a filtered transient pressure above the slab through the joints. For a dynamic pressure as given in Figure 4, and a weak correlation between the pressure acting above and underneath the slab, the response of the liner can be calculated by:

$$u_{max} = C_r \sqrt{2\left[\int_{\omega_1}^{\omega_2} \frac{a_1\,\omega^{n_1}}{(k_e - m\omega^2)^2 + (c_e\omega)^2}\,d\omega + \int_{\omega_2}^{\omega_3} \frac{a_2\,\omega^{n_2}}{(k_e - m\omega^2)^2 + (c_e\omega)^2}\,d\omega + \int_{\omega_c + \frac{\Delta\omega}{2}}^{\omega_c + \frac{\Delta\omega}{2}} \frac{a_3}{(k_e - m\omega^2)^2 + (c_e\omega)^2}\,d\omega\right]} \quad (9)$$

where a_3 is the constant value of the under-pressure PSD. The value may be determined by a prescribed RMS for the dynamic uplift. Solving Equation 9 for different values of the central frequency and bandwidth, the total amplification factor can be obtained. Figure 9 shows the influence of these parameters on the dynamic amplification factor.

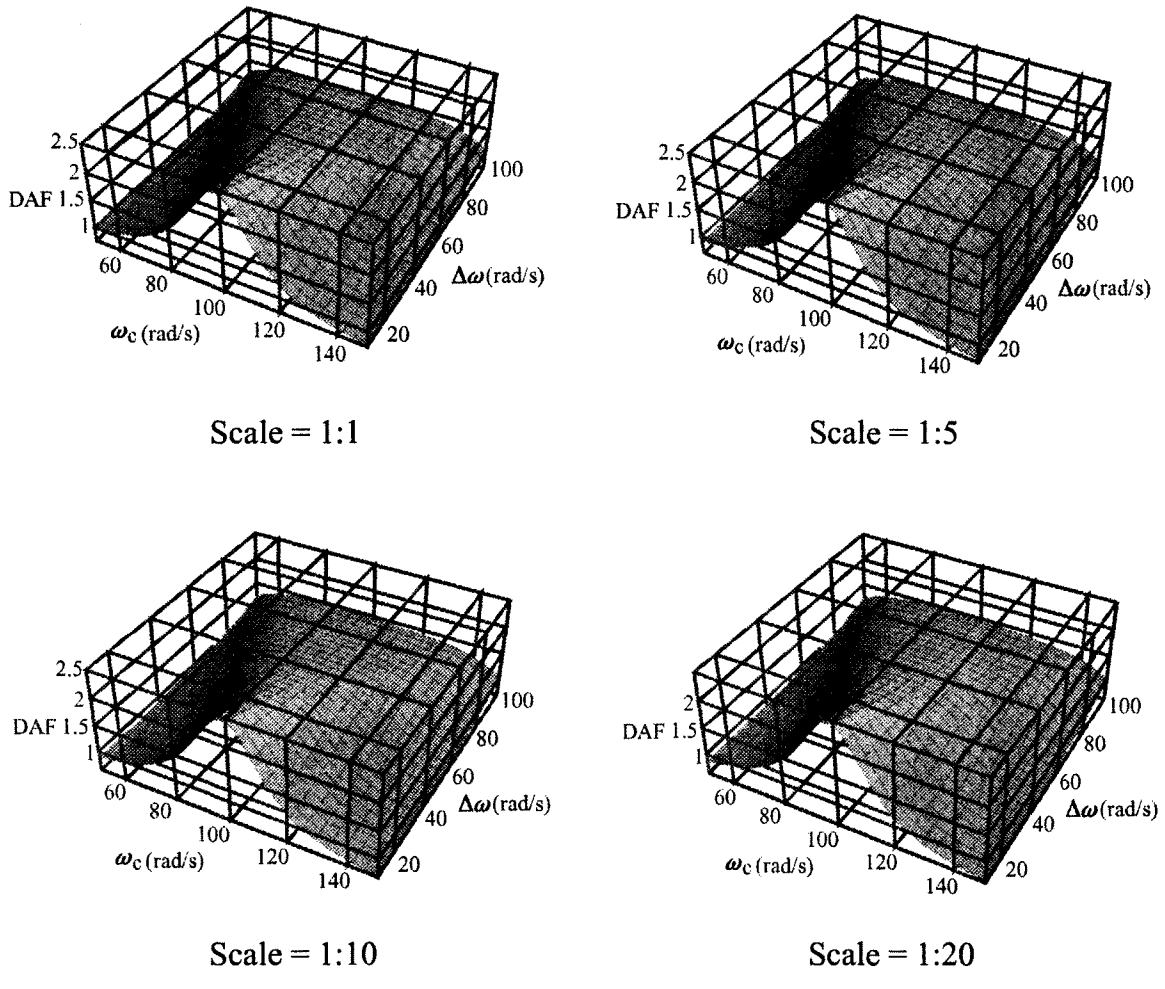

Figure 9. *Variation of the dynamic amplification factor (DAF) as a function of the central frequency, ω_c, of the bandwidth $\Delta\omega$ of the dynamic uplift for different scales*

The most severe condition is obtained for a narrow band pressure with a resonance frequency of the system. The dynamic amplification factor slightly exceeds 2.0, due to the damping associated in the analysis. The results indicate that the use of a dynamic amplification factor of 2.0, as proposed by Fiorotto [8], is somehow conservative. Lower values can be justified from a fully dynamic analysis. The dynamic amplification factor is reduced by the increase of the bandwidth of the under-pressure so that the power is transmitted in a wider frequency range.

5. Design procedure

The design of an anchorage system for plunge pool linings requires both loading and structural modelling. This is due to the high uncertainty associated with both the loading and the system response to pressure fluctuations. The design procedure can be summarised as follows:

1. Acquisition of transient pressure measurements from the hydraulic models is, if possible, near prototype scale, choosing an appropriate sampling rate for catching the high frequency components.
2. Stochastic analysis of the pressure, and evaluation of the PSD and spatial correlation functions.
3. Modelling of the excitation load by proper definition of the PSD and correlation functions, based on the measurement results. The frequency ranges should be selected with care in order to avoid the contribution of components not significant to the prototype conditions.
4. Design of the joint system of the liner.
5. Using simplified random vibration concepts to determine the response and amplification factors with respect to static loading. Several trial sensitivity analyses with various loading models are recommended. The use of simple structural models, as suggested in this paper, is sufficient for the initial design stage. If necessary, more elaborate models can be used, which consider the spatial variation of the pressure fluctuations.
6. Determination of the size and amount of anchors.

6. Conclusion

A stochastic approach was adopted to determine the response of the anchored liner slabs of plunge pools, due to dynamic pressures resulting from high velocity jet impacts. Dynamic amplification factors, defined as the ratio of the dynamic and the static anchor force, were obtained for different assumptions. Furthermore the sensitivity, with respect to excitation frequency, was investigated.

For impervious liners, and a bi-linear loading model with various frequency ranges, amplification factors were observed to be in the range of 5-45%. The results indicated that a static analysis may result in an unsafe design.

For an assumption of identical dynamic pressures above and underneath the slabs, and using the same bi-linear model for PSD of the pressure fluctuations, the amplification factors vary within the range of 5-45%. This is almost the same as expected for the impervious liner.

For a small time lag between the dynamic pressure above and underneath the slabs, dynamic amplification decreases rapidly below unity. This is also expected from the rapid decay of an auto-correlation function of the modelled PSD function.

In the extreme case of a narrow band dynamic uplift, resonance effects can occur with

dynamic amplification factors slightly above 2.0. This can be considered as an upper limit for the amplification value.

List of symbols

$p_1(x,t)$ = Dynamic over-pressure
$p_2(x,t)$ = Dynamic under-pressure
Ω = Spatial distribution averaging factor for the liner segment
M = Mass of the liner segment
c_e = Equivalent damping of the liner segment
k_e = Equivalent linear stiffness of the liner segment
$U(t)$ = Dynamic displacement of the liner segment
$p_1(t)$ = Liner segment spatially averaged over-pressure
$p_2(t)$ = Liner segment spatially averaged under-pressure
$F(t)$ = Force applied to the liner segment
F_0 = Harmonic force amplitude applied to the liner segment
ω = Angular frequency
$S_u(\omega)$ = Power spectral density of dynamic displacement of the liner segment
$S_F(\omega)$ = Power spectral density of the force applied to the liner segment
$H(\omega)$ = Frequency response function
$h(\theta)$ = Impulsive response function
$S_{F_1}(\omega)$ = PSD of the dynamic over-pressure force
$S_{F_2}(\omega)$ = PSD of the dynamic under-pressure force
$S_{F_1F_2}(\omega) = S^*_{F_2F_1}(\omega)$ = Cross-spectral density function between over- and under-pressure force
σ_u = Root mean square value of dynamic displacement of the liner segment
$u_{\max}$ = Maximum dynamic displacement of the liner segment
C_r = Factor associated with the level of the acceptable risk
σ_p = Root mean square value of dynamic pressure (over and/or under)

References

[1] Armengou, J & Ervine, D A, (1991), 'Mean and fluctuating pressure field in full width free nappe stilling basin', *Proceedings*, 24th IAHR Congress, Models & Control System for Hydraulic Engineering, Madrid, Spain, 9-13 September, Vol D, pp261-269.

[2] Bellin, A & Fiorotto,V, (1995), 'Direct dynamic force measurement on slabs in spillway stilling basins', *Journal of Hydraulic Engineering*, ASCE, Vol 121, No 10, pp686-693.

[3] Bollaert, E, (2002), '*Transient water pressures in joints and formation of rock scour due to high-velocity jet impact*', A Schleiss (Ed), Communication No 13 of the Laboratory of Hydraulic Constructions, EPFL, Switzerland, (ISSN 1661-1179).

[4] Bollaert, E, (2003a), 'Scour of rock due to the impact of plunging high velocity jets. Part I: A state-of-the-art review', *Journal of Hydraulic Research*, Vol 41, Issue 5, pp451-464.

[5] Bollaert, E & Schleiss, A, (2003b), 'Scour of rock due to the impact of plunging high velocity jets. Part II: Experimental result of dynamic pressures at pool bottoms and in one- and two-dimentional closed end rock joints', *Journal of Hydraulic Research*, Vol 41, Issue 5, pp465-480.

[6] Bollaert, E, (2004), 'A new procedure to evaluate dynamic uplift of concrete linings or rock blocks in plunge pools', *Proceedings*, Congress on Hydraulics of Dams & River Structures, 26-28 April, Tehran, Iran, pp125-132.

[7] Castillo, L G, (1990), 'Metodología experimental y Numérica para la Caracterización del Campo de Presiones en los Disipadores de Energía Hidráulica. Aplicación al Vertido Libre en Presas de Bóveda,' *PhD thesis*, Universität Politècnica de Catalunya, Barcelona, Spain, [in Spanish].

[8] Fiorotto & Salandin, (2000), 'Design of anchored slabs in spillway stilling basins', *Journal of Hydraulic Engineering*, ASCE, Vol 126, No 7, pp502-512.

[9] Fiorotto, V & Rinaldo, A, (1992), 'Fluctuating uplift and lining design in spillway stilling basins', *Journal of Hydraulic Engineering*, ASCE, Vol 118, No 4, pp578-596.

[10] Häusler, E, (1966), 'Dynamische Wasserdrücke auf Tosbeckenplatten infolge freier Überfallstrahlen bei Talsperren', *die Wasserwirtschaft*, 2, pp42-49, [in german].

[11] Kirschke, D, (1974), '*Druckstoßvorgänge in wassergefüllten Felsklüften*', Institut für Bodenmechanik und Felsmechanik der Universität Fridericiana, Karlsruhe, Heft 61.

[12] Lyatkher, V M & Khalturina, N V, (1962), '*Oscilação de pressão debaixo de uma laje de soleira*', Trudy Gidroposkta, 7, pp30-63, Translation No 525, LNEC.

[13] Melo, J F, Pinheiro, A N & Ramos, C M, (2006), 'Forces on plunge pool slabs: influence of joints location and width', *Journal of Hydraulic Engineering*, Vol 132, No 1, pp49-60. Doi:10.1061/(ASCE) 0733-9429 (2006) 132: 1 (49).

[14] Mirtskhulava, T E, Dolidze, I V & Magomedova, A V, (1967), 'Mechanism and computation of local and general scour in non-cohesive, cohesive soils and rock beds', *Proceedings*, 12th IAAR Congress, pp169-176.

[15] Pinheiro, A N, (1995), 'Acções hidrodinâmicas em soleiras de bacias de dissipação de energia por ressalto', *PhD thesis*, Technical University of Lisbon, Portugal.

[16] Pinheiro, A N & Melo, J F, (2008), 'Effect of jet aeration on hydrodynamic forces on plunge pool floors', *Canadian Journal of Civil Engineering*, Vol 35, pp521-530.

[17] Ramos, C M & Melo, J F, (1992), 'Analysis of hydrodynamic actions in stilling basins under extreme flood conditions - a case study', *Proceedings*, International Symposium on Dams & Extreme Floods, Granada, Spain, Edited by ICOLD.

[18] Townson, J M, (1988), 'The simulated motion of a loose revetment block', *Journal of Hydraulic Research*, Vol 26, Issue 2, pp225-243.

[19] Xu, D M & Yu, C Z, (1983) '*Pressão no fundo de um canal devido ao choque de um jacto plano, e suas características de flutuação*', [Portuguese translation No 841, Laboratório Nacional de Engenharia Civil (LNEC), 1986] Shuili Xuebao, 5: pp52-58.

[20] Yuditskii, G A, (1961), '*Pressões reais no leito, a jusante de barragens de grande altura, com descarregador em salto de esqui*', (in Portugese), LNEC, Lisbon, Translation No 521 of the publication from 'Izvestiya VNII Gidro Tekhniki, Moska', Leningrad, No 67, pp231-240.